



Research article

Research on rice starch gel preparation and crosslink network structure-rheological property based on direct-writing 3D printing

Xuan Xiao^a, Liu Yang^{a,*}, Zilong Xu^a, Pingan Huang^a, Can Shu^a, Shaoyun Song^{a,b}, Yonglin Zhang^{a,b}, Houchang Pei^a

^a College of Mechanical Engineering, Wuhan Polytechnic University, Wuhan, 430048, Hubei, China

^b Hubei Cereals and Oils Machinery Engineering Center, Wuhan, 430048, China

ARTICLE INFO

Keywords:

Rice starch gel
Crosslink network structure
Rheological property
Direct-write 3D printing

ABSTRACT

Amylopectin and amylose components are natural polymers within rice starch granules, intertwined in specific conditions to form gel polymerized with pore crosslink network, has potential printing properties. In this study, a rice starch gel preparation scheme is proposed for stable properties, and starch granule phase transition mechanism is analyzed based on RVA test during preparation, it can be divided into four-stage, swelling, reacting, homogenizing and self-assembling stages. Gel surface tension and contact angle tested with starch concentration effect, a correlation is developed, reflecting a competition result to gel droplet macro-morphology between the intermolecular cohesion and crosslink network. SEM is used to reveal typical crosslink structures of different starch molecular component proportions, providing objective support for starch gel rheologic property change. Results indicate gel interior crosslink network formed under concentration 12 %, the gel with amylose 4.475 % presents better printing accuracy. Gel shear modulus positively correlated with amylose proportion. Japonica gel under 20 % is of higher viscosity and rapid reassembly ability after interior crosslink network is broken. Max dynamic viscosity is positively correlated with starch concentration. The study aims to provide theoretical and practical support for in-depth analysis of rice starch material application in direct-write 3D printing.

1. Introduction

Additive manufacturing (AM), compared with traditional material reduction manufacturing or forming manufacturing, is an advanced manufacturing technology that adds printing material layer by layer to products building, presenting significant advantages to manufacturing complex parts on efficiency and responsiveness, and it is applied in many fields, including aerospace technology, biomedical and food engineering [1,2]. Factually, as one of AM, direct-writing 3D printing based on inkjet technology has attracted large attention, enhancing people's quality of life [3,4]. In personalized food processing field, based on specific rheological properties, the gel phase printing ink can be extruded through a specific nozzle, forming three-dimensional solids layer-by-layer buildup, which is crucial for the application of rice starch gel in direct-write 3D printing [5,6].

Rice starch granule, a natural and abundant natural polymer, is a hydrolysis product of brown rice endosperm. It is formed by the polymerization of amylopectin and amylose molecules, with large amount of glucose [7,8]. Meanwhile, the research indicates starch

* Corresponding author.

E-mail address: yangliu@wpu.edu.cn (L. Yang).

<https://doi.org/10.1016/j.heliyon.2024.e24057>

Received 9 August 2023; Received in revised form 28 November 2023; Accepted 3 January 2024

Available online 4 January 2024

2405-8440/© 2024 Published by Elsevier Ltd.

This is an open access article under the CC BY-NC-ND license
















(<http://creativecommons.org/licenses/by-nc-nd/4.0/>).

granules can form a polymer gel under specific conditions by phase transition, and certain plasticizers added can improve the starch gel-relevant mechanical property, receiving large attention [9]. However, in-depth research from the biomechanical perspective is lacking on the printability of pure rice starch granules. It is a fundamental research point for rice starch gel printability exploration, leading the realization of starch gel personalized printing.

In previous research, the printability capability of other natural starches has been investigated by researchers, focusing on effects of starch concentration, plasticizer proportion and gel rheological property [10,11]. Noted that viscoelasticity of potato and cassava gels showed significant change with increasing starch concentration, enhancing the starch gel flowing stress and storage modulus [12]. The xanthan gum addition can improve the starch gels extrudability and printing accuracy, which was verified by the method of computational fluid dynamics simulation. The gelatinized starch gel reheating leads to a decrease in strength, hardness and elasticity [13,14]. Meanwhile, in rice starch gel research, the squeezability and structural recovery rate of rice starch gel improved after adding cate-chins. The gel rheology and freeze-thaw stability were affected, the viscoelastic property was improved [15,16]. However, the application of pure rice starch gels is lacking in direct-write 3D printing. The gel droplet macro-morphology formation has not been studied, and gel interior cross-linked structures formed by starch molecular forming proportion are not revealed. The potential mechanics model is not established between typical crosslink structure and starch concentration. Therefore, based on intermolecular and crosslinked network of rice starch gel, rice starch gel printability in direct 3D printing still needs systematic and deep analysis.

In order to obtain rice starch gels with stable printing properties, a preparation scheme was proposed based on RVA testing, rice starch phase transition mechanism was revealed to verify the validity of preparation scheme. The relationship between rice starch gel surface tension and starch concentration was analyzed, and a correlation was established. The rice starch gel contact angle form was analyzed from the perspective of intermolecular and mechanics. Meanwhile, SEM image reveals structural types of cross-linked networks within starch gel under different starch molecule component proportions, affecting the gel mechanics properties. In addition, starch gel shear strength was analyzed, and a potential logic was presented between shearing power law and gel flow behavior. The current limitation was noted that rice gel flow model cannot be accurately built, and the relevant stability of crosslink structure lacks analysis under the oscillatory testing, which is important to explore gel polymerization. The results can provide new research methodology and theoretical guidance for rice starch gel in direct-writing 3D printing.

Table 1
All prepared rice starch gel samples.

Starch type	4%	8%	12%	16%	20%
Japonica gel					
Indica gel					
Glutinous gel					

2. Materials and methods

2.1. Experimental material

In the study, three typical pure rice starch (Wuxi Jinnong Biotechnology Co., Ltd., China) are chosen to avoid the physicochemical effects of other substances. Japonica starch (amylose 17.9 %), indica starch (amylose 19.43 %), glutinous starch (amylose 5.32 %), are critical to the establishment of constitutive relation between testing and the analysis of crosslinking network microstructure. They were purchased for the laboratory in April 2023 and stored in a drying environment. The amylose proportion within three rice starch granules is determined by professional testing institution (Eurofins Analytical Technology Services Co., Ltd., France).

2.1.1. Preparation process

Preparation purpose: the rice starch gels prepared have well-printable properties, including stable state, full of gelatinized and formed crosslinking network within gel [17]. Therefore, based on the viscosity evolution behavior analysis of three rice starch in section 3.1, a rice starch gel preparation scheme with scientific was proposed for food 3D printing. During preparation, a certain weight rice starch granules and deionized water were weighed into the beaker, preparing the starch gel sample with different concentrations. Then, the beaker was placed in water bath at 50 °C, 320 rpm. The mixture solution was driven by a magnetic stirrer, providing sufficient impact energy to ensure that rice starch granules completed the phase transition in deionized water. After 13 min, when the water bath temperature increased to 90 °C, the beaker was taken out and immersed into the water at room temperature 25 ± 1 °C for 300 s. Rice starch gel was obtained with stability finally (all samples shown in Table 1). Fig. 1 shows the schematic diagram of rice starch gel preparation in the study.

2.2. Experimental device and details

2.2.1. RVA (rapid viscosity analyzer) measurement

RVA, a research methodology, is used to analyze the fluid viscosity evolution behavior under the combined influence of temperature and time. In the study, a rapid viscosity analyzer (Porton Ruihua Scientific Instruments Co., Ltd., Sweden) was used to reveal the phase transition mechanism of three rice starches, which was important to guide the preparation process of starch gel in section 4.2. Before test, rice starch 3 g and deionized water 25 g were weighed into equipment stirring chamber, a constant 160 rpm was set. The temperature program was set. The dynamic viscosity with three rice starch solutions was recorded during test under different temperature conditions [18]. The specific analysis of RVA data is shown in section 3.1.

2.2.2. Surface tension and three-phase contact angle measurement

The study uses an optical contact angle calculation instrument (Shanghai Zhong-cheng Digital Technology Equipment Co., Ltd., China) to measure the contact angle and surface tension of rice starch gel prepared. Before measurement, the syringe of diameter 0.7 mm was adopted, a glass slide was selected as the solid interface, density difference 0.998 g/cm³ was set. During measurement, syringe with an appropriate amount of starch gel was fixed on the equipment, droplet control bolt was slowly adjusted to make starch gel gradually extruded, forming a state of static equilibrium. A droplet image was captured to calculate the surface tension by pendant drop method [19]. Further, image of starch gel drop falling on the interface was captured to calculate the contact angle by angle measuring.

Fig. 2 shows the schematic diagram and calculation principle of contact angle equipment. Equation (1) is the kernel model of pendant drop method, θ is starch gel con-tact angle.

$$2 - \frac{R_1 \times \Delta\rho \times g}{\gamma} \times \left(\frac{y_2}{R_1} \right) = \frac{R_1}{R_2} + \frac{R_1 \times \sin \alpha}{X_2} \quad (1)$$

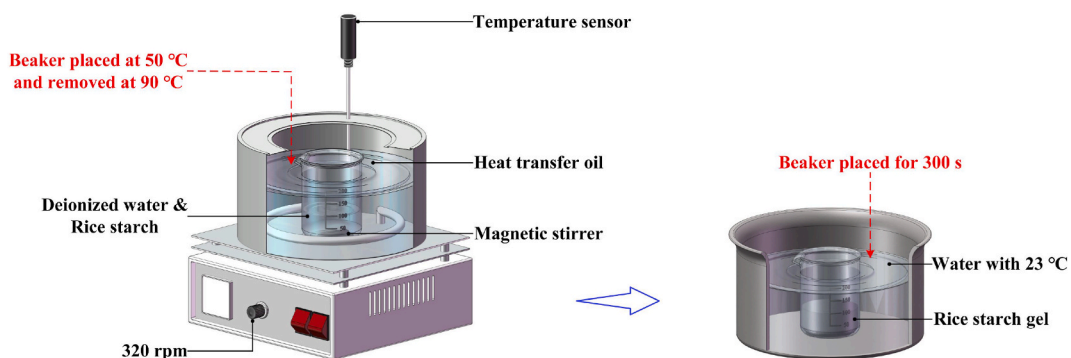


Fig. 1. Schematic diagram of rice starch gel preparation.

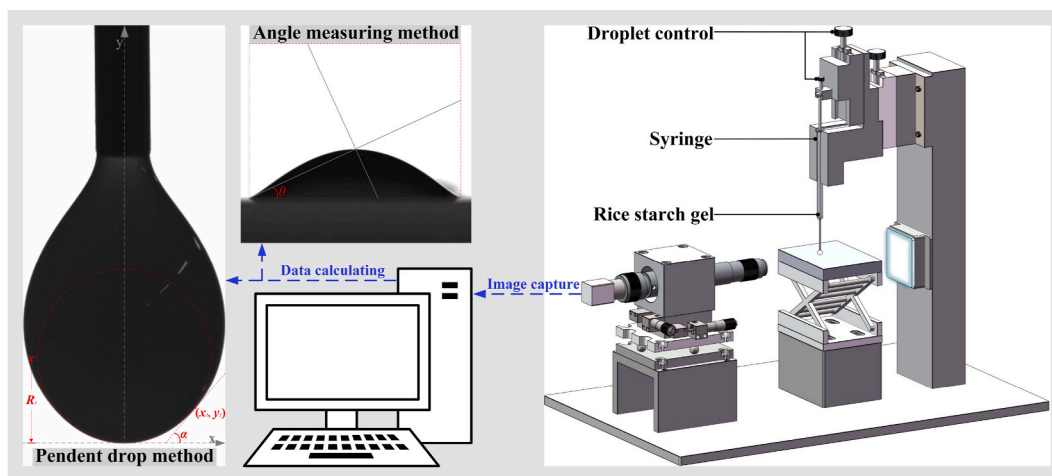


Fig. 2. Schematic diagram and calculation principle of contact angle equipment.

where γ is surface tension of starch gel, R_1 is curvature radius at the droplet bottom, g is gravitational acceleration, R_2 is the main curvature radius at point (x_2, y_2) , $\Delta\rho$ is density difference in the air, 0.998 g/cm^3 .

2.2.3. Rheological measurement

The study used a rotational rheometer (RH-20; Shanghai Baosheng Industrial Development Co., Ltd., China) to characterize the mechanical properties of rice starch gel prepared, including rigidity, stability and flowability. Before testing, the parallel plate with diameter 50 mm was used. Starch gel was placed on the test platform with 1 mm gap. Meanwhile, shear rate 0.1 to 100 s^{-1} was set to obtain stable shear viscosity in the flow test, the angle frequency 1.5 – 150 rad/s and constant strain 5% was set in the oscillation test. During measurement, starch gel dynamic viscosity η and shear modulus G were recorded, analyzing the mechanical properties of physical crosslinking network within the gel.

2.2.4. Microstructure characterization

SEM, an instrument of observation, is used to characterize the material microscopic morphology and to analyze the microregion composition. In the study, the crosslink network structure of starch gel samples was observed by a field emission scanning electron microscope (FESEM; Hitachi S-4800), operated at an accelerating voltage 5.0 kV . Before shooting, all rice starch gel was freeze-dried for 72 h and fixed on the sample platform with conductive adhesive [20]. Then, the starch gel was sprayed with gold. During shooting, the samples were observed with suitable microscope magnifications.

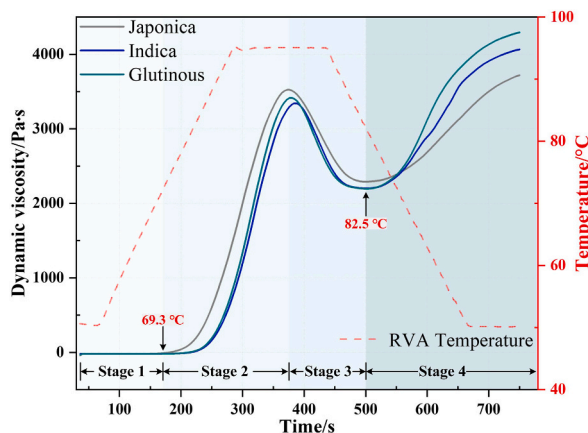


Fig. 3. RVA (Rapid Viscosity Analyzer) curves of three rice starch granules.

3. Result and discussion

3.1. Phase transition of rice starch granules

In direct-write 3D printing, the printing ink needs to be fluid, ensuring the ink extruded through the nozzle under certain pressure. The extruded ink requires well-mechanical properties [21]. Rice starch granule is solid-phase and is hardly compatible with water in nature. The two-phase solution is not printable, indicating the importance of phase transition work for rice starch success printing. Fortunately, under specific temperatures and sufficient water molecules, the rice starch granule semi-crystalline structure is dissolved. Starch molecules (amylopectin and amylose) move and assemble liberally from ordered structure to disordered, forming a gel with crosslink internal molecule structure, which is the starch phase transition [22].

Intrinsically, the phase transition of starch granules is due to hydrogen bonds between starch molecules robbed by water molecules. The starch molecules micro-crystalline bundle structure gradually disintegrated, resulting in more hydrogen bonds forming between water and amylose molecules. Meanwhile, free water molecules gathered toward starch molecules outside by hydration, promoting the transition from multi-phase solution to gel phase condition with stability. Furthermore, with environment temperature decreasing, the ability vanishes of water molecules to rob the hydrogen bonds between starch molecules, the hydration decreases. Self-assembly between starch molecules begins with hydrogen bonds, forming a physical crosslink network three-dimension structure. Finally, large number of water molecules are locked in the network gap, and the rice starch gel with stable viscoelasticity is condensed and formed [23].

The rice starch gel rapid viscosity was tested. Fig. 3 shows the RVA curves of three rice starch, providing theoretical support for the starch phase transition. Test result indicates the dynamic viscosity evolution matches with the structure. It can be divided into four-

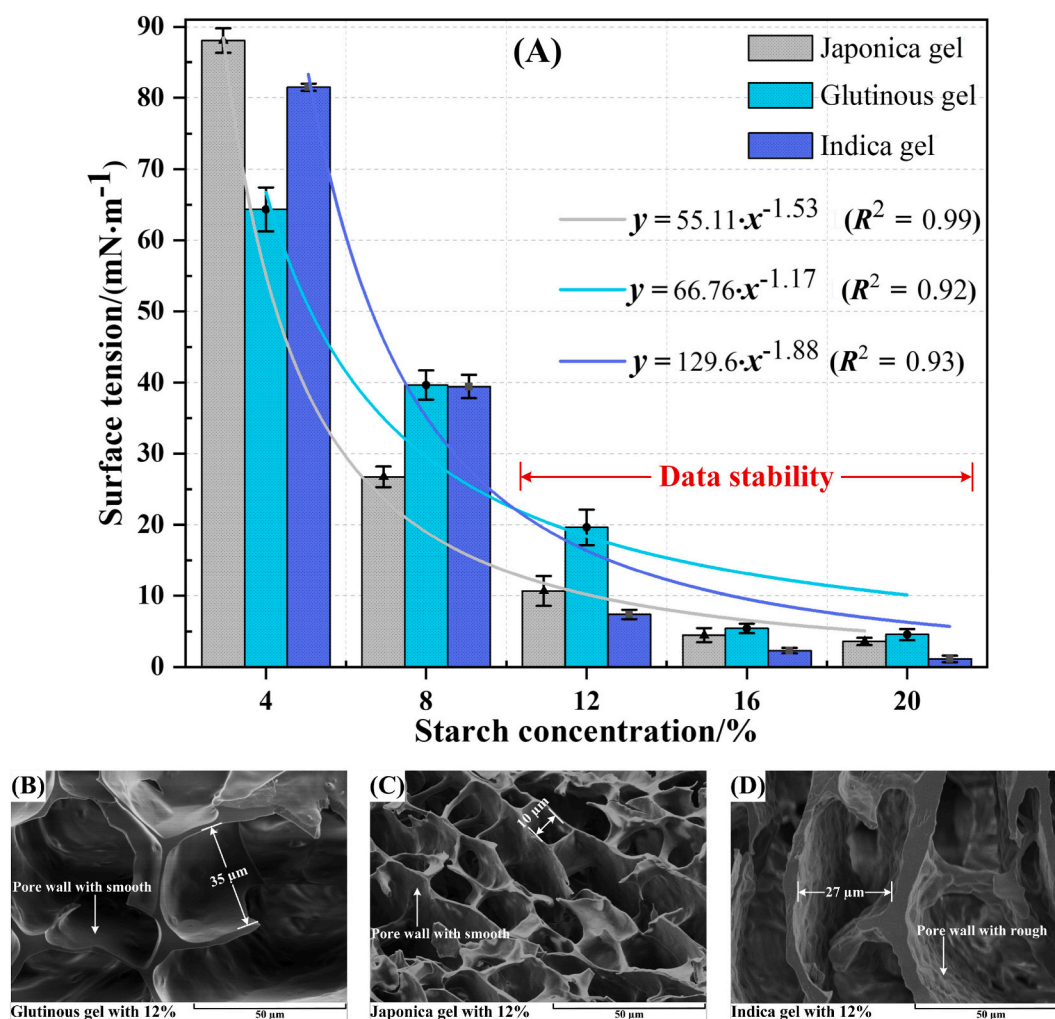


Fig. 4. (A) Concentration effect on three rice gel surface tension; (B)–(D) Gel Crosslink network structure under concentration 12 %: (B) glutinous gel, (C) japonica gel, (D) indica gel.

stage, swelling, reacting, homogenizing, self-assembly stage, matching the starch phase transition in deionized water. Firstly, swelling stage, the starch granule volume gradually increases, small amount of amylose is released into the solvent from starch granule interior. The solution viscosity stables, and it presents two distinct phases (solid phase starch granule, liquid phase solvent). Secondly, reacting stage, the starch granule volume continues expanding and squeezing each other with temperature increasing. Larger number of new hydrogen bonds begin forming between amylose and water molecules in the solution. Intermolecular friction chance increases in the small area, leading to a rapid increase in dynamic viscosity. Thirdly, homogenizing stage, the dominant effect of external thermal energy decreases, starch granule disappears after the volume expands to limit, the solution starts to transform from multi-phase to homogeneous gel, and more hydration reduces the chance of intermolecular friction in small area, resulting in a short-term decrease in dynamic viscosity. Fourthly, self-assembly stage (retrogradation stage), the hydrogen bonds are broken between starch and water molecules with temperature decreasing, new hydrogen bonds are formed and cross-linked between starch molecules. Meanwhile, large crosslink group is interwoven to form a three-dimensional physical crosslinking network. Water molecule is located in the network gap, the solution fluidity reduced, leading viscosity increase and gradually stabilized with the crosslink network structure.

3.2. Macro-morphology properties of rice starch gel

3.2.1. Surface tension

Surface tension, reflecting the ability of droplet surface to be contracted, is the liquid inherent property. It is determined by interior intermolecular forces [24]. In single-phase flow, surface tension is a macroscopic reflection of interior cohesion, indicating the ability to attract each other between same molecule. As natural polymer, rice starch gel surface tension is co-determined by intermolecular force and interior crosslink network. It is the result of two intersections for starch gel surface tension, which is important for improving the theoretical base about various gel surface tension and further research in numerical simulation.

Fig. 4A shows surface tension with concentration the effect on three kinds rice starch. The result indicated that gel surface tension is negatively correlated with starch concentration. The evolution is stable after concentration 12 %, and finally converged, demonstrating the crosslinked network formed within rice gel. Under starch concentration 4 %, the small crosslink network is dispersed within gel system. The cohesion between water molecules dominates droplet mechanical property, resulting in glutinous gel with large molecular weight presenting smaller surface tension (under same starch concentration, large of amylopectin proportion shows larger molecular weight). Under starch concentration 8 %, the crosslink network structure is formed within japonica and glutinous gel, and large amounts of amylose hinder the formation of stable crosslink network structure of indica gel. Under starch concentration 12 %, as shown in Fig. 4B–D, the crosslink network structure is formed within three starch gels. The glutinous gel network structure presents large pores with smooth walls (typical size 35 μm). The friction chance between molecules is small, and water molecules can better exist in large pores. The droplet macro-morphology is not completely controlled by interior cross-link network structure. The japonica gel network structure shows small pores with smooth walls (size 10 μm), the cohesion-forming ability between water molecules is smaller than large pores. Interior crosslink network forms a better control of the droplet macro-morphology compared with glutinous gel. The network structure of indica gel presents large pores with rough walls (typical size 27 μm), and larger pore wall thickness, cohesion formation between water molecules is difficult in pores. The chance of intermolecular friction is large in small areas, resulting in the droplet macro-morphology being controlled by interior crosslink network. Under starch concentrations 16 %–20 %, interior crosslink network structure controls the three starch gels droplet macro-morphology. Finally, it is stable and surface tension converges (glutinous gel > japonica gel > indica gel). In addition, the three starch gel surface tension is fitted in detail with equation model (2).

$$y = a \cdot x^b \quad (2)$$

where a is the constant of regularization, b is the scaling exponent (the model is negative allometry when $b < 1$), x is starch concentration, and y is the surface tension of rice gel.

The fitting models are $y = 55.11 \cdot x^{-1.53}$ ($R^2 = 0.99$) japonica gel, $y = 66.76 \cdot x^{-1.17}$ ($R^2 = 0.92$) glutinous, and $y = 129.6 \cdot x^{-1.88}$ ($R^2 = 0.93$) indica. In the established model. Three starch gels regularization constant a is the intrinsic coefficient, and the surface tension reducing rate is determined by the scaling exponent b ($a < b$ indicating rapid reduction rate). Indica gel shows smallest scaling exponent ($b = -1.88$), with surface tension reducing rate fast, indicating the droplet macro-morphology affected by the crosslink network structure within indica starch gel. From intermolecular forces, the amylose molecular proportion is 19.43 % in indica starch granules, leading to the cohesion formation between water molecules being hindered, due to the amylose robbing by water molecules during phase transition. Furthermore, in self-assembly stage, the hydrogen bonds cannot form rapidly between dispersed water molecules. The crosslink network structure can be assembled quickly, and more amyloses are cohered to the formed network structure, resulting in the thick and rough pore wall formation (shown in Fig. 4D), which affects the changing rate of starch gel surface tension. The fitted curve indicates that rice starch gel surface tension is affected by interior crosslink network structure, including network forming rate, pore form and starch molecular component proportion.

3.2.2. Three-phase contact angle

The contact angle, characterizing the droplet profile on a solid interface, is a physical parameter of interaction degree between liquid and solid. Large contact angle expresses well-hydrophobicity in the study of pure liquid phase, reflecting the energy relationship between intermolecular cohesion and adhesion from liquid macro-morphology perspective [25].

During direct-write 3D printing, the printed first ink layer needs a well-contact for maintaining the product overall printing accuracy and formability. Contact angle is an important parameter needs calibration in printing droplet numerical simulation,

characterizing the interaction between different molecules on macroscopic scale. It is a basis for establishing intermolecular mechanical model. In the research, rice starch gel under different concentrations is not a pure phase. Its macro-morphology is co-determined by interior crosslink network structure and molecule interaction, indicating the basic point of starch gel contact angle is crosslink network effect on droplet morphology [26].

Fig. 5A shows the three rice starch gels contact angle under different concentrations, and in situ images of japonica gel. Test result indicates rice starch gel contact angle is positively correlated with concentration effect. Japonica and indica gel contact angle show a linear increase before concentration 16 %. Glutinous gel contact angle presents an irregular increase and starts to stabilize after 16 %, starch concentration 16 % ($\theta > 140^\circ$) is turning point for the rice starch gel macro-morphology. It can be analyzed from the perspective of crosslink network structure state within gel. Under starch concentration 4 %, the small crosslink network block is dispersed in solution, structural support is not formed. Gel droplet lacks formability (shown in in-situ image). The glutinous gel presents larger contact angle, indicating amylopectin molecules proportion contributes to the connection between cross-link networks under low concentration. Under starch concentration 8 %, the formed interior crosslink network starts to support gel droplet macro-morphology, and indica gel contact angle presents a high increase rate, indicating the gel droplet macro-morphology is dominated effectively by more amylopectin or amylose. Under starch concentration 12 %, the crosslink network structure formed within three starch gels. The internal pore can provide support for the gel droplet morphology. Starch gel starts to be endowed with well-formability, which is the basis for direct-write 3D printing. Under starch concentration 16 %, three starch gel contact angles all reached 145° , a better morphology formed for gel droplets. The contact angle started to converge. Concentration 16 % is turning point for crosslink network structure. Under starch concentration 20 %, all sample contact angle is stable, meaning higher starch concentration no longer affects the contact angle of starch gel. The macro-morphology presents better accuracy than 16 %. In addition, japonica gel forming accuracy is the best under same contact angle during test. It can be analyzed from the perspective of rice starch gel crosslink network structure.

Fig. 5B–D shows SEM images of crosslink network structure of three rice starch gels under concentration 20 %. The results indicate rice starch gel with different amylose proportions presents a multi-crosslink network structure, an important point for self-assembly

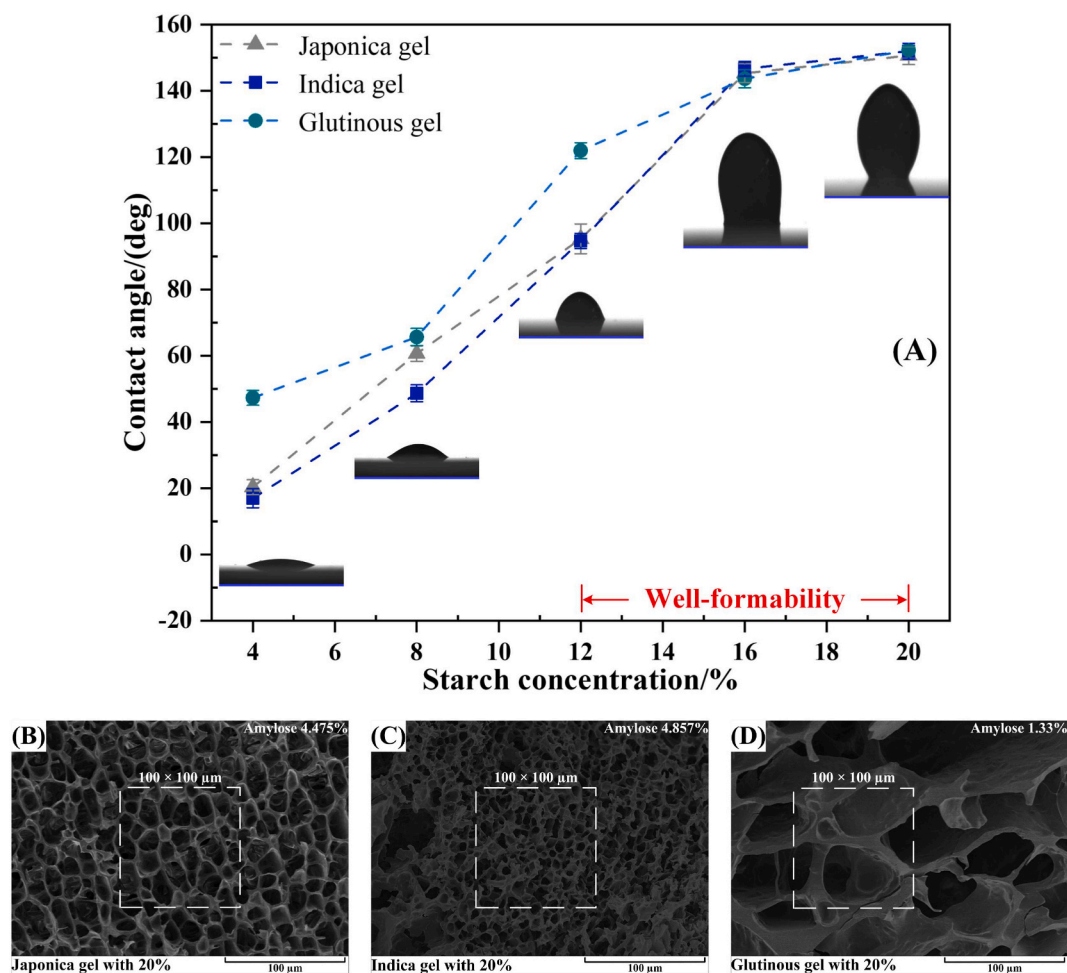


Fig. 5. (A) Three rice starch gels contact angle under different concentrations and in situ image on japonica gel; (B)–(D) SEM images of gel crosslink network structure under concentration 20 %: (B) japonica gel, (C) indica gel, (D) glutinous gel.

behavior of starch molecules. In $100 \times 100 \mu\text{m}$ view, japonica gel pore structure well self-assembly in the crosslinked network (amylose 4.475 %). The pore formation is homogeneous, and edge connections between pores tend to be 120° (a stable triangular structure in nature). Indica gel crosslink network of presented regularity (amylose 4.857 %), resembling the japonica gel network structure, with smaller and more dense pores. The crosslinked network of glutinous gel presents a larger pore size and thicker pore wall (amylose 1.33 %), resulting in a more layered crosslink network. Based on contact angle curve and SEM image, both typical crosslink network structures can support the gel droplet macro-morphology, forming a stable contact angle. The stable macro-morphology does not reflect the mechanical and viscoelastic properties of rice starch gel, further analysis is needed.

3.3. Rheological properties of rice starch gel

3.3.1. Shear strength

Shear modulus, characterizing the material ability to resist deformation, is a basic rheological property. Large modulus presents higher material rigidity, the greater bonding force between the smallest material units from a microscopic view [27]. Superficially, the internal bonding force of rice starch gels mainly originates from the hydrogen bonds between starch molecules (amylopectin and amylose molecule), and the cohesion between water molecules is also a critical bonding force under low starch concentration. Rice starch molecules are natural macromolecules. Crosslink network structure can form by self-assembly during phase transition, dominating gel mechanics property. It is important for the material constitutive model establishing and molecular dynamics simulation. In rice starch gel mechanics study, the interior crosslink network structure is a critical factor in gel rigidity analysis.

During direct-write 3D printing, the printing ink with high-shear modulus presents a well-ability of deformation resistance and tolerates more shear forces, which is needed for overall printing product layer and accuracy [28]. In order to measure the shear modulus of rice starch gel, a rotational rheometer is used. It determines various mechanics parameters while the crosslinked structure is broken within polymer gel. Analyzing the rigidity of three rice starch gels under different starch concentrations. Equation (3) is introduced to calculate the starch gel shear modulus.

$$G = \tau \cdot \gamma^{-1} \tag{3}$$

where G is the shear modulus of rice starch gel, τ is shear stress while the crosslinked structure is broken, and γ is shear strain.

Fig. 6A shows the concentration effect on the rice starch gel shear modulus. The curve indicates shear modulus of japonica and indica gel is positively correlated with starch concentration. Glutinous gel presents an unrelated trend with increasing starch concentration, indicating the gel rigidity is affected by starch molecule component proportion in the solution (shown in Fig. 6B). Under starch concentrations 4 % and 8 %, the crosslink network structure is not completely formed within the gel. The mechanical properties are dominated by the cohesion between water molecules, leading no significant changes in rigidity of three rice starch gels. Under starch concentration 12 %, basic crosslink network is formed within the gels. The shear modulus starts to change essentially. The shear modulus of japonica and indica gels present an obvious difference, due to the close starch molecular component proportion. Glutinous gel shows stable shear modulus under low and high concentrations. With starch concentration from 16 % to 20 %, the shear modulus of japonica and indica gels gradually increased. The modulus difference is stable, showing a positive correlation between gel rigidity and starch concentration under specific starch molecule component proportions (glutinous gel molecule proportion does not meet the correlation). The glutinous gel shear modulus is not affected by testing concentrations, the modulus is stable with $2500\text{--}2700 \text{ N}\cdot\text{m}^{-2}$, showing poor rigidity. Noted that glutinous gel amylose proportion is lower in the solution than other two rice starch, indicating amylose proportion is positively correlated with rice starch gel rigidity. It needs further analysis from the perspective of crosslink network structure.

Fig. 7 shows SEM images of glutinous gel crosslink structure from starch concentration 8 %–20 %. Structure images indicate that

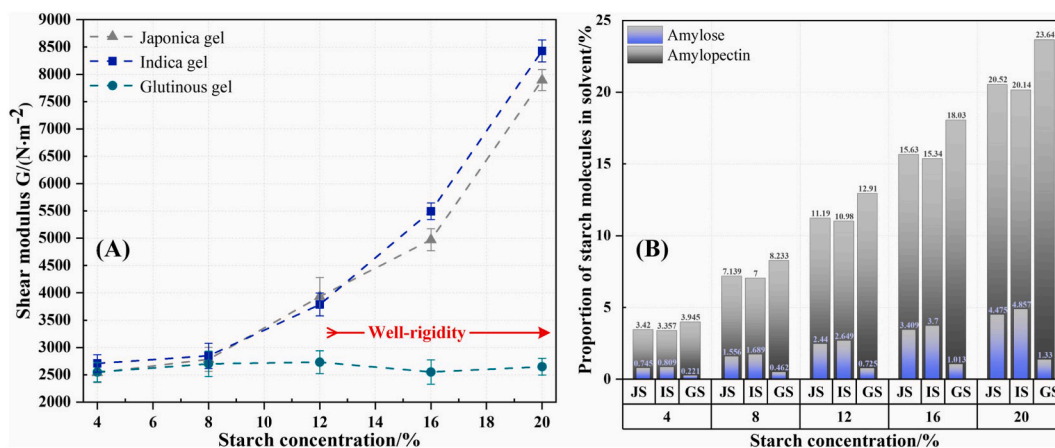


Fig. 6. (A) Concentration effect on rice starch gel shear modulus; (B) Starch molecule component proportion (amylopectin and amylose) in the solvent.

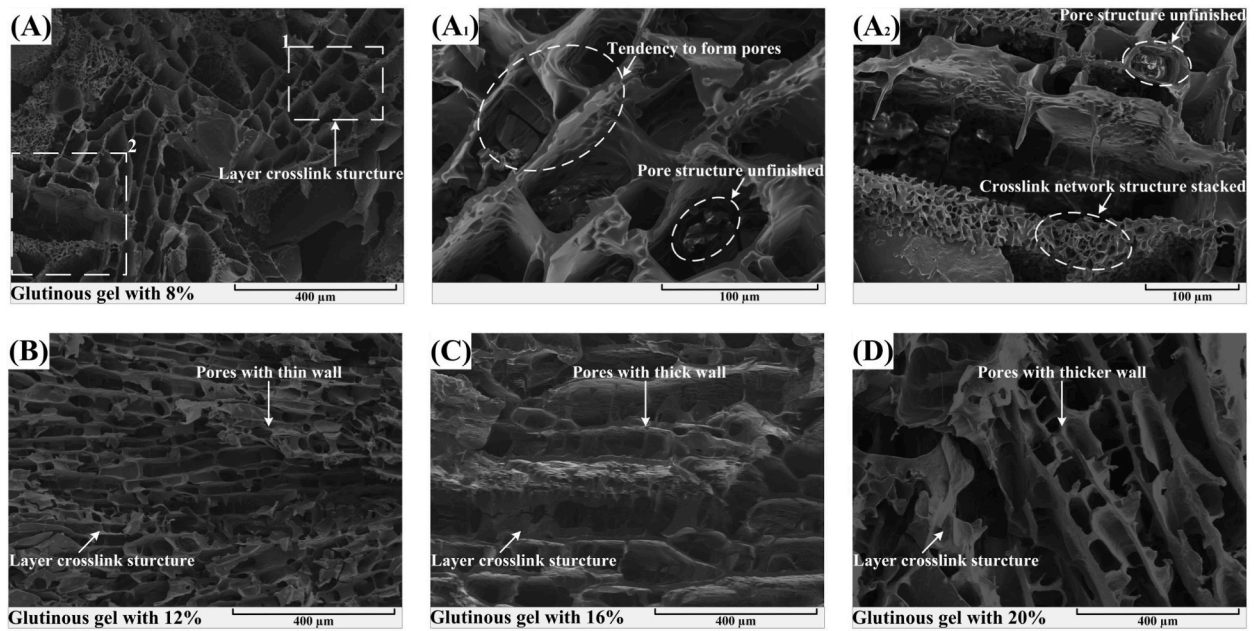


Fig. 7. SEM images of glutinous gel crosslink network: (A) starch concentration 8 %, (B) 12 %, (C) 16 %, (D) 20 %.

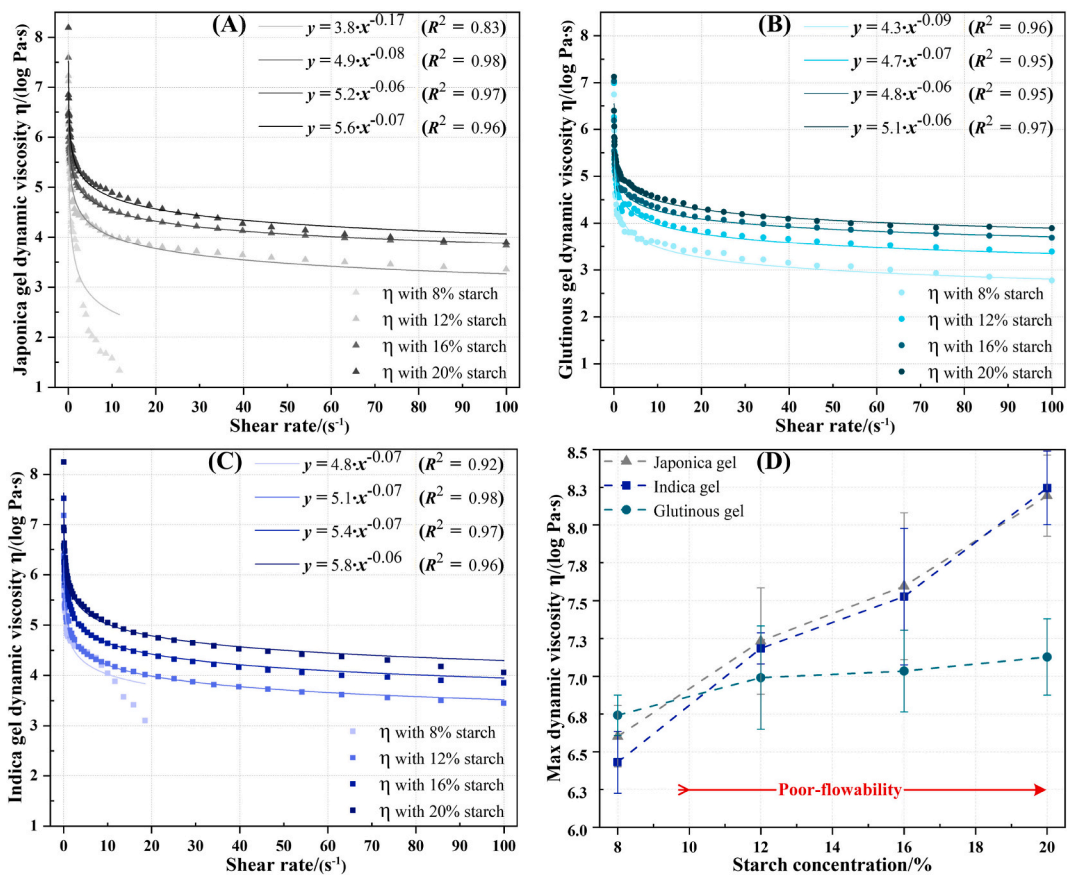


Fig. 8. Shear rate effect on three gel dynamic viscosity under different starch concentrations: (A) japonica gel, (B) glutinous gel, (C) indica gel; (D) Starch concentration effect on maximum dynamic viscosity of three rice starch gels.

the gel crosslink network presents a layer crosslink structure with all samples, differing the crosslink network of japonica and indica gels. It is caused by different starch molecule component proportions. Under starch concentration 8 %, as shown in Fig. 7A₁ and A₂, the regular crosslink network is not completely formed within gel, and pores with incomplete walls are filled in the crosslink layer. The tendency of pores formation and the stacked crosslink network can be clearly observed in certain small areas. Under starch concentration 12 %, as shown in Fig. 7B, the complete layer crosslink structure is formed within gel. All pores have regular and uniform, thin pore walls, producing maximum glutinous gel shear modulus $2699 \text{ N}\cdot\text{m}^{-2}$. With starch concentration increasing (Fig. 7C–D), the pores size and pore walls gradually increased based on the unchanged layer crosslink structure. Gel shear modulus is not promoted. Based on the shearing modulus and SEM image above, the rice starch gel crosslink structure is influenced by starch molecules (amylopectin and amylose) proportion in the solution. It further reflects on the starch gel mechanical property. Noted that crosslink network presents the glutinous gel layer structure with high proportion amylopectin molecule. The pore and pore wall dimension are positively correlated with starch concentration, producing poor rigidity than japonica and indica gels.

3.3.2. Flow characteristic analysis

Dynamic viscosity, reflecting the viscosity ability, is an intrinsic property of fluid and viscoelastic material. It is co-determined by the intermolecular forces and crosslink network structure within the material. In non-Newtonian fluid, with shear rate changing, the material viscosity is changed. Pseudoplastic fluid viscosity decreased with increasing shear rate, presenting the shear thinning phenomenon. It is needed in direct-write 3D printing [29]. Typically, in polymer gel, the dynamic viscosity change is consistent with the pseudoplastic behavior, due to the network structure broken velocity being faster than it is reorganized. The viscosity change is described by the power-law equation in one-dimensional directional flow, shown in equation (4).

$$\eta = k \cdot \dot{\gamma}^n \quad (4)$$

where η is the gel dynamic viscosity, k is consistency coefficient (larger k means the higher the viscosity), n is the non-Newtonian index, reflecting crosslink network's reorganization ability within the gel after broken.

In direct-write 3D printing, with printing ink passing through the nozzle, its velocity is changed due to mass conservation, leading to the viscosity change of print ink (non-Newtonian fluid). Based on the actual printing requirement, it is important to print index of the high viscosity at zero shear stress and faster reorganization ability of interior crosslink network [30]. Rice starch gel flow characteristics need to be analyzed deeply and systematically. It is a basis for the application of rice starch gel in direct-write 3D printing.

Fig. 8A–C shows the shear rate effect on the dynamic viscosity of three rice starch gels under different starch concentrations. The result indicates three starch gel viscosity change is consistent with pseudoplastic fluid properties under all concentrations, presenting shear thinning property. Noted the japonica and indica gels dynamic viscosity decreased rapidly under concentration 8 %, due to interior crosslink network is not formed. As shown in Fig. 8A, with starch concentration increasing, the gel dynamic viscosity gradually increases under same shear rate. The consistency coefficient increased from 4.9 to 5.6. It indicates the starch concentration with stable rate growth can reduce starch gel flowability. The gel non-Newtonian index with 20 % is -0.07 , smaller than concentration 16 %, indicating japonica gel high viscosity under starch concentration 20 %. It has the ability to reorganize rapidly after crosslink network structure is broken, presenting an outstanding property for printable ink in direct-writing 3D printing. As shown in Fig. 8C, the indica gel dynamic viscosity evolution law is similar to japonica gel. Increasing cardinal number of consistency coefficient is the same (from 4.9 to 5.6), indicating existence a correlation between starch gel consistency coefficient and the starch molecules proportion in solution (unclear whether gel consistency coefficient is specifically affected by amylopectin or amylose molecular). Noted that indica gel non-Newtonian index is larger than japonica gel under concentration 20 % ($-0.06 > -0.07$). The crosslink network with stable triangular structure has better reassembly ability after broken. As shown in Fig. 8B, the increasing range of glutinous gel consistency co-efficient is obviously small with starch concentration increasing (from 4.3 to 5.1), leading the gel well flowability. Its non-Newtonian index gradually increased (from -0.09 to -0.06), showing the reassembly ability of layer crosslink structure is negatively correlated with starch concentration, which needs to be avoided in direct-write 3D printing.

Fig. 8D shows the starch concentration effect on maximum dynamic viscosity of three rice starch gels, reflecting the gel viscosity at zero shear stress. It is an important parameter that needs to be calibrated. Test result indicates the gel maximum dynamic viscosity is positively correlated with starch concentration. Correlation coefficient of japonica and indica gel is larger than glutinous gel. From starch concentration 8 %–20 %, the japonica and indica gel viscosity η present competing increase with a small region, indicating the gel maximum dynamic viscosity model can't be established by a simple correlation between the coefficient and non-Newtonian index. It is co-determined by the gel mechanic parameter and interior crosslink network structure. Noted that glutinous gel viscosity η increase rate is smaller than other two starch gels (from 6.8 to 7.2), leading better flowability under same starch concentration. It is caused by the special layer crosslink structure within glutinous gel (120° stable triangular structure load capacity bigger than layer crosslink structure in structural mechanics).

4. Conclusion

In this study, a preparation scheme based on RVA testing is proposed to obtain rice starch gel with stable properties, revealing rice starch granule phase transition is the result of hydrogen bond transfer between starch and water molecules. RVA results indicate the viscosity change can be divided into four-stage, swelling, reacting, homogenizing and self-assembling stage, matching the starch phase transition. The gel droplet macro-morphology formation mechanism is analyzed deeply from the bio-structure mechanics perspective, and the crosslinked network is initially formed within all gel under starch concentration 12 %, meaning the surface tension is stable

(glutinous gel > japonica gel > indica gel). SEM images and the fitted data indicate the crosslinked network affects gel surface tension, including network form rate, pore form and starch molecule component proportions. Glutinous gel presents a layer crosslink structure (amylose 0.221 %–1.33 %). Meanwhile, based on rice gel rheological behavior, a potential logical relationship is proposed between crosslink structure and starch gel model parameters. Glutinous gel shear modulus presents an uncorrelated trend with starch concentration, indicating gel rigidity is positively correlated with the amylose proportion. The dimension of pore and pore wall is positively correlated with starch concentration, producing poorer rigidity. Gel dynamic viscosity changes match with the pseudoplastic fluid property, showing shear thinning. Japonica gel with concentration 20 % has high viscosity and well-reorganize ability after interior network structure is broken. Layer crosslinked structure reorganization ability is negatively correlated with starch concentration. Insight into future study scope, optimizing the printability of rice gel by promoting intermolecular crosslinking, establishing the intrinsic relationship between gel and printing nozzle by numerical simulation, which can form systematic research methodology for natural polymer in direct-write 3D printing.

Data availability statement

Data will be made available on request.

CRediT authorship contribution statement

Xuan Xiao: Conceptualization, Data curation, Formal analysis, Investigation, Methodology, Software, Visualization, Writing – original draft. **Liu Yang:** Funding acquisition, Methodology, Project administration, Resources, Validation, Visualization, Writing – review & editing. **Zilong Xu:** Software, Supervision. **Pingan Huang:** Software, Supervision. **Can Shu:** Software, Supervision. **Shaoyun Song:** Funding acquisition, Investigation, Software, Supervision. **Yonglin Zhang:** Software, Supervision. **Houchang Pei:** Supervision, Validation.

Declaration of competing interest

On behalf of the co-authors, we declare that we have no financial and personal relationships with other people or organizations that can inappropriately influence our work. There is no professional or other personal interest of any nature or kind in any product, service and/or company that could be construed as influencing the position presented in, or the review of, the manuscript entitled “**Research on rice starch gel preparation and crosslink network structure-rheological property based on direct-writing 3D printing**”.

Acknowledgments

The study is mainly funded by Youth Project of Natural Science Foundation of Hubei Province (No. 2022CFB944), Science and Technology Research Project of Hubei Provincial Education Department (No. Q20211609), Key R&D plan of Hubei Province (No. 2022BBA0047), part of the research is supported by Jiangsu Key Laboratory of Advanced Food Manufacturing Equipment & Technology (FM-202103), Hubei Provincial grain bureau project and the Science Foundation of Wuhan Polytechnic University (No.2019RZ08, 2020J06).

Appendix A. Supplementary data

Supplementary data to this article can be found online at <https://doi.org/10.1016/j.heliyon.2024.e24057>.

References

- [1] K. Zampouni, C.K. Mouzakitis, A. Lazaridou, T. Moschakis, E. Katsanidis, Physicochemical properties and microstructure of bigels formed with gelatin and κ -carrageenan hydrogels and monoglycerides in olive oil oleogels, *Food Hydrocolloids* 140 (2023) 108636–108647.
- [2] S.H. Siddique, P.J. Hazell, H. Wang, J.P. Escobedo, A.A. Ameri, Lessons from Nature: 3D Printed Bio-Inspired Porous Structures for Impact Energy Absorption–A Review, *Additive Manufacturing*, 2022, pp. 103051–103077.
- [3] S. Kang, W. Liu, J. Wang, H. Song, W. Yuan, C. Huang, Self-adaptive 3D lattice for curved sandwich structures, *Addit. Manuf.* 54 (2022) 102761–102777.
- [4] M. Shahbazi, H. Jäger, R. Ettelaie, Kinetic evaluation of the starch molecular behavior under extrusion-based or laser powder bed fusion 3D printing systems: a systematic structural and biological comparison, *Addit. Manuf.* 57 (2022) 102934–102945.
- [5] Z. Cai, M. Li, F. Zhang, Y.Z. Li, W.T. Ye, X.W. Fan, Impact of lignin on the starch accumulation, composition, and pasting properties of cassava, *LWT* (2023) 115073–115113.
- [6] N. Hu, C. Zhao, S. Li, W. Qi, J. Zhu, M. Zheng, J. Liu, et al., Postharvest ripening of newly harvested corn: structural, rheological, and digestive characteristics of starch, *LWT* 180 (2023) 114728–114736.
- [7] Z. Shao, Y. Song, Y. Hong, S. Tao, J. Sun, C. Liu, L. Cao, et al., The extension of vacuum microwave drying time improved the physicochemical properties, in vitro digestibility and antioxidant activity of brown rice flour, *LWT* (2023) 115023–115031.
- [8] A. Aleixandre, C.M. Rosell, Starch gels enriched with phenolics: effects on paste properties, structure and digestibility, *LWT* 161 (2022) 113350–113360.
- [9] O. Yuliarti, E. Gusti, J.H. Chiang, P.X. Teo, J.Y. Ng, Rheological and microstructural properties of native cassava starch-low methoxyl pectin in a fruit filling gel system, *LWT* 146 (2021) 111568–111572.
- [10] S.A. Alias, N. Mhd Sarbon, Rheological, physical, and mechanical properties of chicken skin gelatin films incorporated with potato starch, *npj Science of Food* 3 (1) (2019) 26–35.

- [11] S. Wang, C. Li, L. Copeland, Q. Niu, S. Wang, Starch retrogradation: a comprehensive review, *Compr. Rev. Food Sci. Food Saf.* 14 (5) (2015) 568–585.
- [12] R.R. Mauro, A.J. Vela, F. Ronda, Impact of starch concentration on the pasting and rheological properties of gluten-free gels. Effects of amylose content and thermal and hydration properties, *Foods* 12 (12) (2023) 2281–2300.
- [13] Y. Cui, C. Li, Y. Guo, X. Liu, F. Zhu, Z. Liu, F. Yang, et al., Rheological & 3D printing properties of potato starch composite gels, *J. Food Eng.* 313 (2022) 110756–110766.
- [14] J. Jiang, J. Li, W. Han, Q. Yang, Q. Liu, H. Xiao, Y. Fang, et al., Effects of reheating methods on rheological and textural characteristics of rice starch with different gelatinization degrees, *Foods* 11 (21) (2022) 3314–3328.
- [15] X. Zeng, T. Li, J. Zhu, L. Chen, B. Zheng, Printability improvement of rice starch gel via catechin and procyanidin in hot extrusion 3D printing, *Food Hydrocolloids* 121 (2021) 106997–107006.
- [16] X. Xu, S. Ye, X. Zuo, S. Fang, Impact of guar gum and locust bean gum addition on the pasting, rheological properties, and freeze–thaw stability of rice starch gel, *Foods* 11 (16) (2022) 2508–2524.
- [17] N. Carvajal-Mena, G. Tabilo-Munizaga, M. Pérez-Won, C. Herrera-Lavados, R. Lemus-Mondaca, L. Moreno-Osorio, Evaluation of physicochemical properties of starch-protein gels: printability and postprocessing, *LWT–Food Sci. Technol.* 182 (2023) 114797–114808.
- [18] Y. Pei, Y. Zheng, Z. Li, J. Liu, X. Zheng, K. Tang, D.L. Kaplan, Ethanol-induced coacervation in aqueous gelatin solution for constructing nanospheres and networks: morphology, dynamics and thermal sensitivity, *J. Colloid Interface Sci.* 582 (2021) 610–618.
- [19] J. Wen, D. Dini, H. Hu, E.R. Smith, Molecular droplets vs bubbles: effect of curvature on surface tension and Tolman length, *Phys. Fluids* 33 (7) (2021).
- [20] Y. Yue, J. Liu, S. Gao, Y. Pei, Y. Jiang, K. Tang, X. Zheng, et al., Ionically conductive gelatin-based hybrid composite hydrogels with high mechanical strength, self-healing, and freezing-tolerant properties, *Eur. Polym. J.* 172 (2022) 111230–111239.
- [21] V. Nguyen-Van, S. Li, J. Liu, K. Nguyen, J.P. Tran, Modelling of 3D Concrete Printing Process: A Perspective on Material and Structural Simulations, *Additive Manufacturing*, 2022, pp. 103333–103383.
- [22] M. Xu, S. Ji, Y. Li, J. Li, Y. Liu, K. Li, B. Lu, Exploring the mechanism of variation in 3D printing accuracy of cassava starch gels during freezing process, *Food Hydrocolloids* 140 (2023) 108657–108670.
- [23] X.M. Han, J.J. Xing, X.N. Guo, K.X. Zhu, Effects of extruded endogenous starch on the gel-entrapped network formation in gluten-free Tartary buckwheat noodles during sheeting, *LWT* 160 (2022) 113226–113234.
- [24] T.J. Teleszewski, A. Gajewski, The latest method for surface tension determination: experimental validation, *Energies* 13 (14) (2020) 3629–3639.
- [25] P. Roy, S. Liu, C.S. Dutcher, Droplet interfacial tensions and phase transitions measured in microfluidic channels, *Annu. Rev. Phys. Chem.* 72 (2021) 73–97.
- [26] H. Yu, Y.C. Jin, W. Cheng, X. Yang, X. Peng, Y. Xie, Multiscale simulation of atomization process and droplet particles diffusion of pressure-swirl nozzle, *Powder Technol.* 379 (2021) 127–143.
- [27] X. Li, Z. Hu, Y. Wang, C. Qin, Z. Xu, X. Chen, Y. Wang, et al., Microscopic mechanism study of the rheological behavior of non-Newtonian fluids based on dissipative particle dynamics, *Soft Matter* 19 (2) (2023) 258–267.
- [28] R.D. Corder, Y.J. Chen, P. Pibulchinda, J.P. Youngblood, A.M. Ardekani, K.A. Erk, Rheology of 3D printable ceramic suspensions: effects of non-adsorbing polymer on discontinuous shear thickening, *Soft Matter* 19 (5) (2023) 882–891.
- [29] N. Wang, Y. You, X. Liao, F. Zhang, J. Kan, J. Zheng, Ultrasonic Modification of lotus Starch Based on Multi-Scale Structure: Pasting, Rheological, and Thermal Properties, *LWT*, 2023, pp. 115030–115040.
- [30] Y. Hou, J. Zhao, J. Yin, F. Geng, S. Nie, The synergistic gelation of *Dendrobium officinale* polysaccharide (Dendronans) with xanthan gum and its rheological and texture properties, *Food Hydrocolloids* 141 (2023) 108674–108683.